Antideuteron and antihelium cross sections for cosmic-ray studies

Diego Gomez

Department of Physics & Astronomy
University of Hawaii at Manoa
dgomezco@hawaii.edu

XSCRC workshop
CERN Nov 2019

Indirect search for dark matter

Expected antideuteron production in cosmic-ray interactions

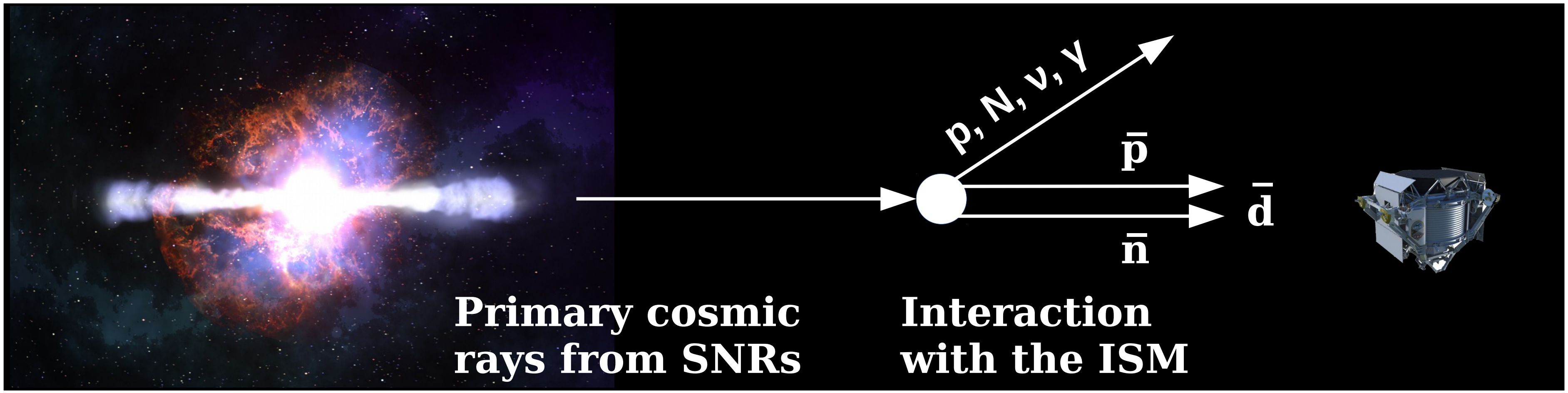

Hypothetical antideuteron cosmic-rays from dark matter

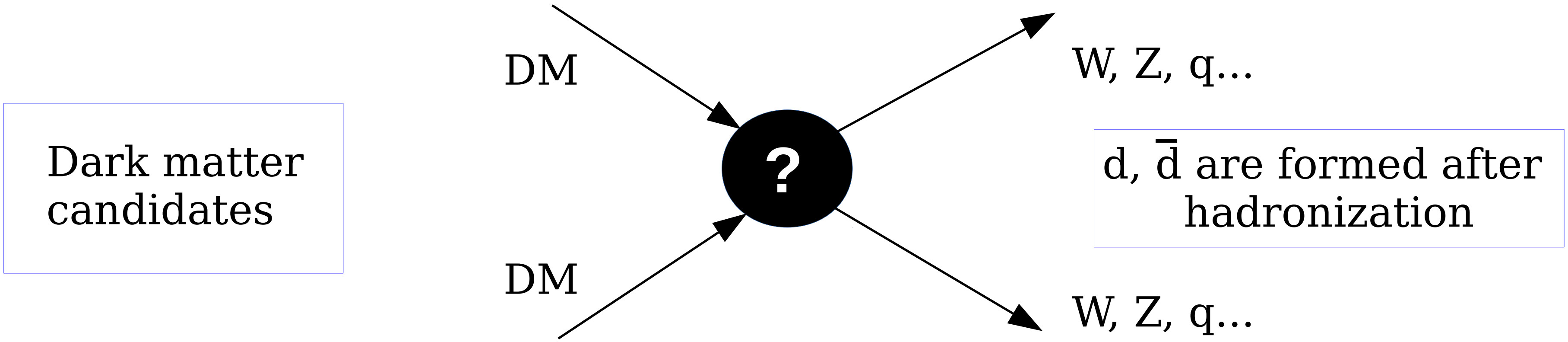

Indirect search for dark matter

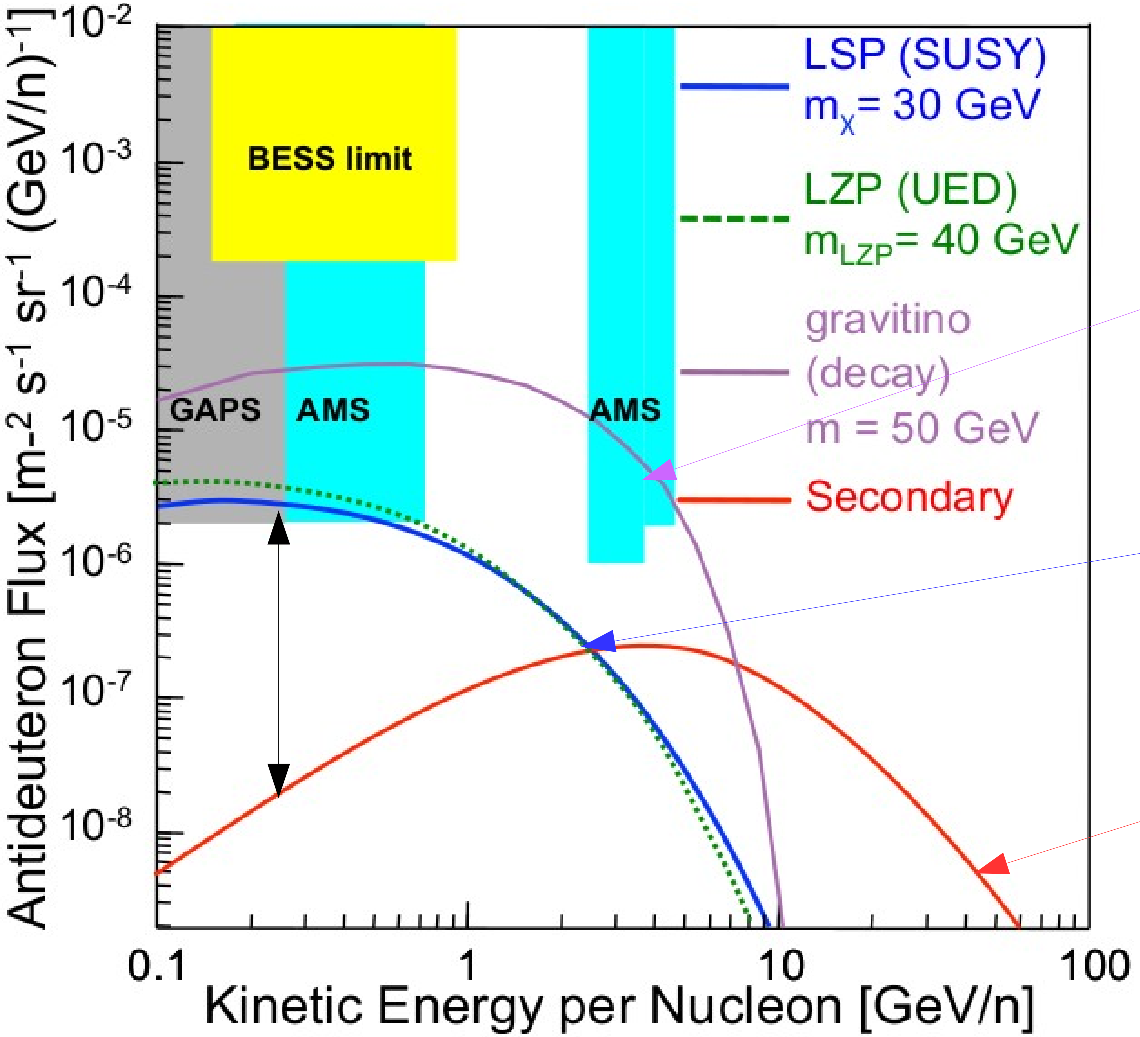

Examples of antideuteron signals from dark matter candidates interactions.

Late decays of unstable gravitinos

Neutralino:
SUSY lightest supersymetric particle, decay into bb

Astrophysical background:
Cosmic-ray collisions with the interstellar medium

Antideuterons are an important unexplored indirect detection technique.

T. Aramaki et al., Phys. Rept. 618, 1 (2016), arXiv:1505.07785 [hep-ph].

Antideuteron formation model

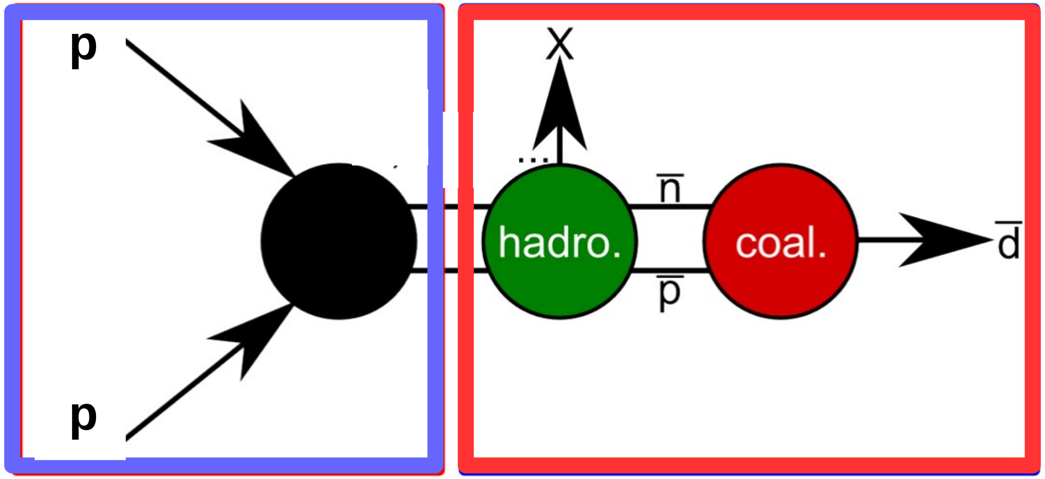

p+p, p+He, He+p, pbar+p collisions

Coalescence

Coalescence Model

Deuterons and antideuterons can be formed by a pair p-n or $\overline{p}$-$\overline{n}$ close in phase space.

$$\gamma_d \frac{d^3N_d}{dp_d^3} = \frac{4\pi}{3} p_0^3 \left(\gamma_p \frac{d^3N_p}{dp_p^3}\right)\left(\gamma_n \frac{d^3N_n}{dp_n^3}\right)$$

p_0 is extracted from this comparison

Collisions are simulated with **Monte Carlo** generators

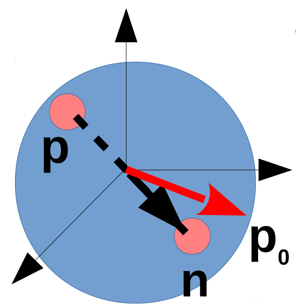

Afterburner

d and $\overline{d}$ are created from the pairs **event by event**

The results from simulations are compared to data

Antiproton production simulation

- To generate a correct prediction of antideuterons using MC, it is necessary to have a proper description of antiprotons.

Experiment or Laboratory	Reference	Collision	Final states	p_{lab} (GeV/c)	$\sqrt{s}$ (GeV)
ITEP [1]	[192]	p+Be	p	10.1	4.5
CERN [1]	[193, 194]	p+p	p, $\bar{p}$	19.2	6.1
		p+Be	p, $\bar{p}$		
CERN [1]	[194]	p+p	p	24	6.8
NA61/SHINE	[195]	p+C	p	31	7.7
	[85]	p+p	p, $\bar{p}$		
NA61/SHINE	[85]	p+p	p, $\bar{p}$	40	8.8
Serpukhov [1]	[196, 197]	p+p	p, $\bar{p}$	70	11.5
	[198]	p+Be	p, $\bar{p}$		
	[199]	p+Al	p, $\bar{p}$		
NA61/SHINE	[85]	p+p	p, $\bar{p}$	80	12.3
CERN-NA49	[82]	p+p	p, $\bar{p}$	158	17.5
	[83]	p+C	p, $\bar{p}$		
CERN-NA61	[85]	p+p	p, $\bar{p}$		
CERN-SPS [1]	[200, 201]	p+Be	p, $\bar{p}$	200	19.4
		p+Al	p, $\bar{p}$		
Fermilab [1]	[202, 203]	p+p	p, $\bar{p}$	300	23.8
		p+Be	p, $\bar{p}$		
Fermilab [1]	[202, 203]	p+p	p, $\bar{p}$	400	27.4
		p+Be	p, $\bar{p}$		
CERN-ISR	[204]	p+p	p, $\bar{p}$	1078	45.0
CERN-ISR	[204]	p+p	p, $\bar{p}$	1498	53.0
CERN-LHCb	[86]	p+He	$\bar{p}$	6.5×10^3	110
CERN-ALICE	[84]	p+p	p, $\bar{p}$	4.3×10^5	900
CERN-ALICE	[84]	p+p	p, $\bar{p}$	2.6×10^7	7000

Proton and antiproton data list on p+p and p+A collisions to be compared to simulations. **D. Gomez-Coral et al. Phys. Rev. D 98, 023012 (2018) arXiv:1806.09303 [astro-ph.HE]**

Invariant differential cross section for **antiprotons** in p+p collisions at 158 GeV/c, as function of rapidity

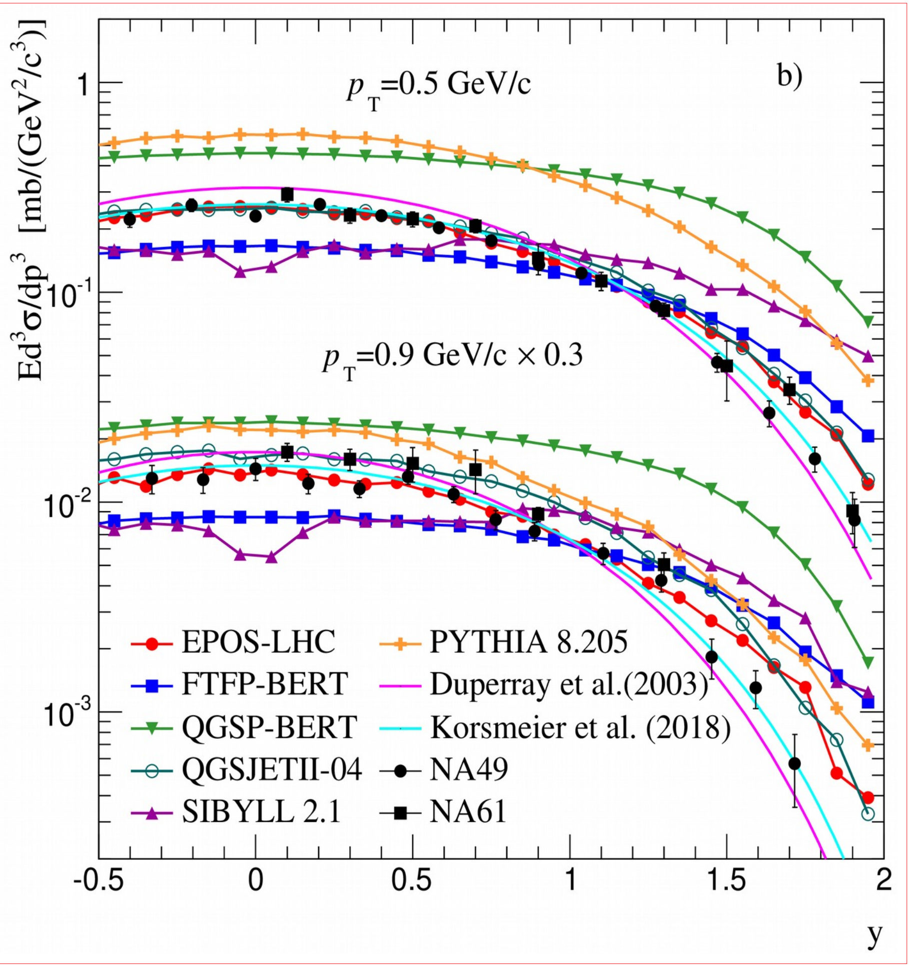

Antiproton production simulation

- Simulation is compared to data point by point.
- The most reliable MC model is selected from the comparison to data.

$$\frac{\Delta}{\epsilon_\Delta} = \frac{\left(E\frac{d^3\sigma}{dp^3}^{sim} - E\frac{d^3\sigma}{dp^3}^{data}\right)}{\sqrt{(\epsilon_{sim})^2 + (\epsilon_{data})^2}}$$

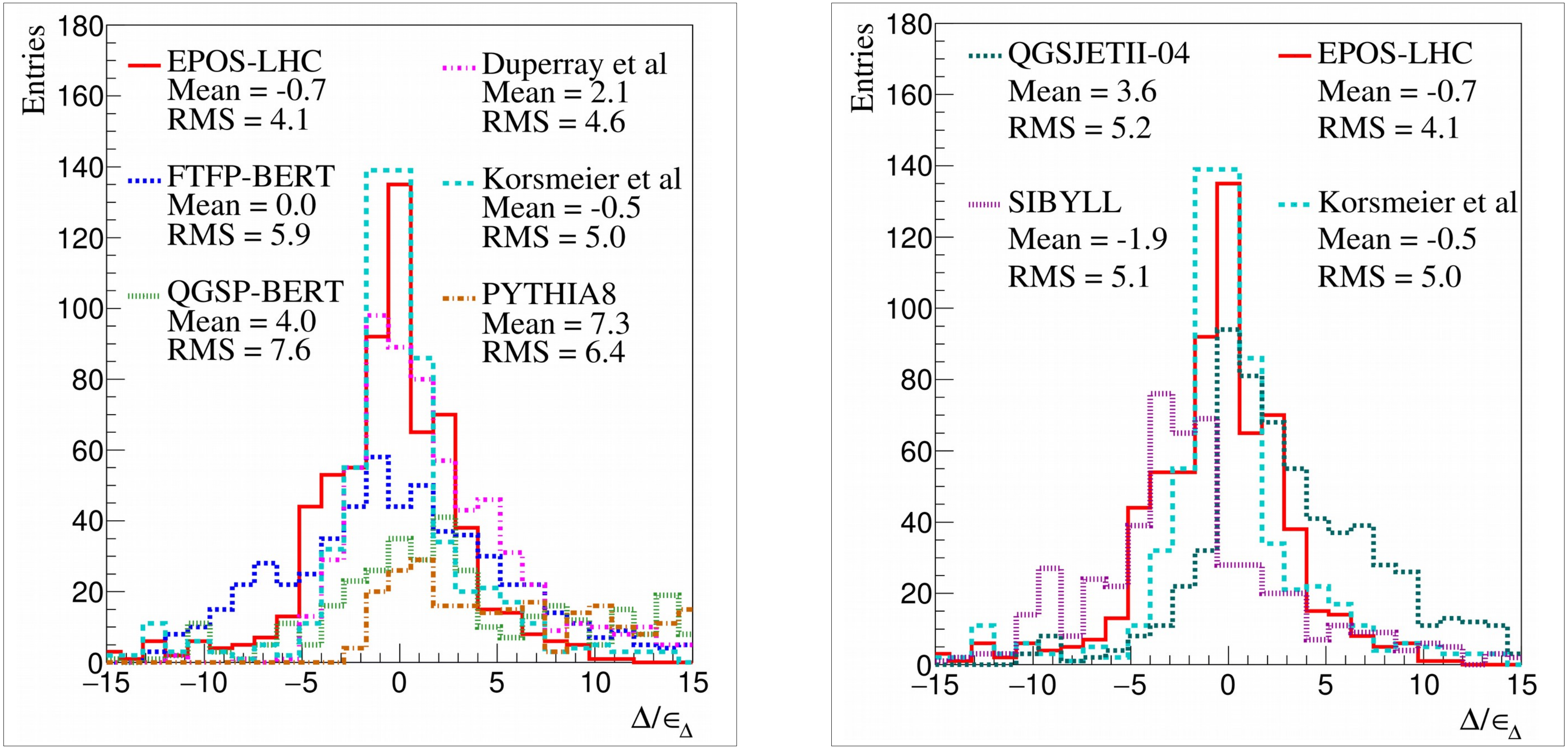

Antideuteron production simulation

- The coalescence momentum (p_0) is determined from the fit of simulations to data.

Experiment or Laboratory	Reference	Collision	p_{lab} (GeV/c)	$\sqrt{s}$ (GeV)	No. of points d	No. of points dbar
CERN	[194]	p+p	19	6.15	6	0
CERN	[194]	p+p	24	6.8	4	0
Serpukhov	[198]	p+p	70	11.5	7	2
CERN-SPS	[200, 205]	p+Be	200	19.4	6	3
		p+Be			3	5
		p+Al			3	3
Fermilab	[203]	p+Be	300	23.8	4	1
CERN-ISR	[206, 207, 208]	p+p	1497.8	53	3	8
CERN-ALICE	[155, 209]	p+p	4.3×10^5	900	3	3
CERN-ALICE	[155, 209, 210]	p+p	2.6×10^7	7000	21	20

Deuteron and antideuteron data list on p+p and p+A collisions to be compared to simulations. **D. Gomez-Coral et al. Phys. Rev. D 98, 023012 (2018) arXiv:1806.09303 [astro-ph.HE]**

p+p at √s = 11.5 GeV

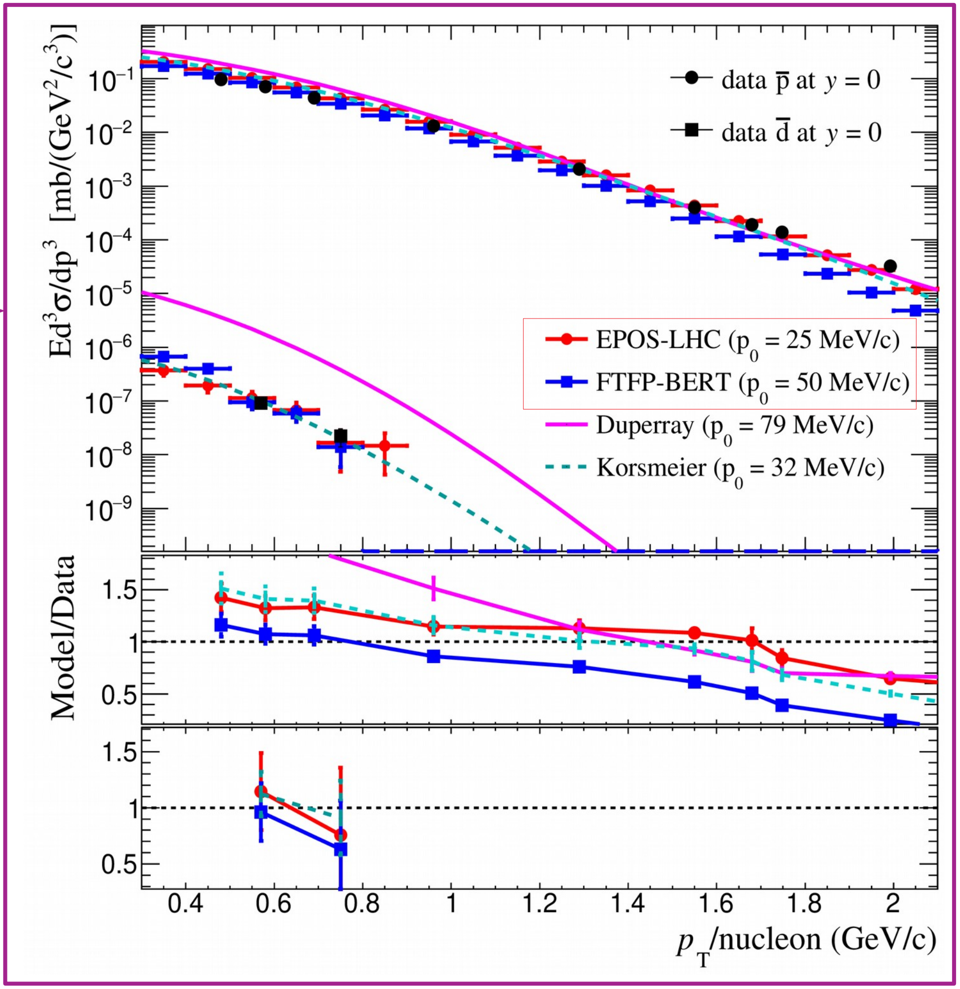

Antideuteron invariant differential cross section in p+p collisions at 70 GeV/c, as function of p_T

Antideuteron production simulation

p+p at √s = 53 GeV

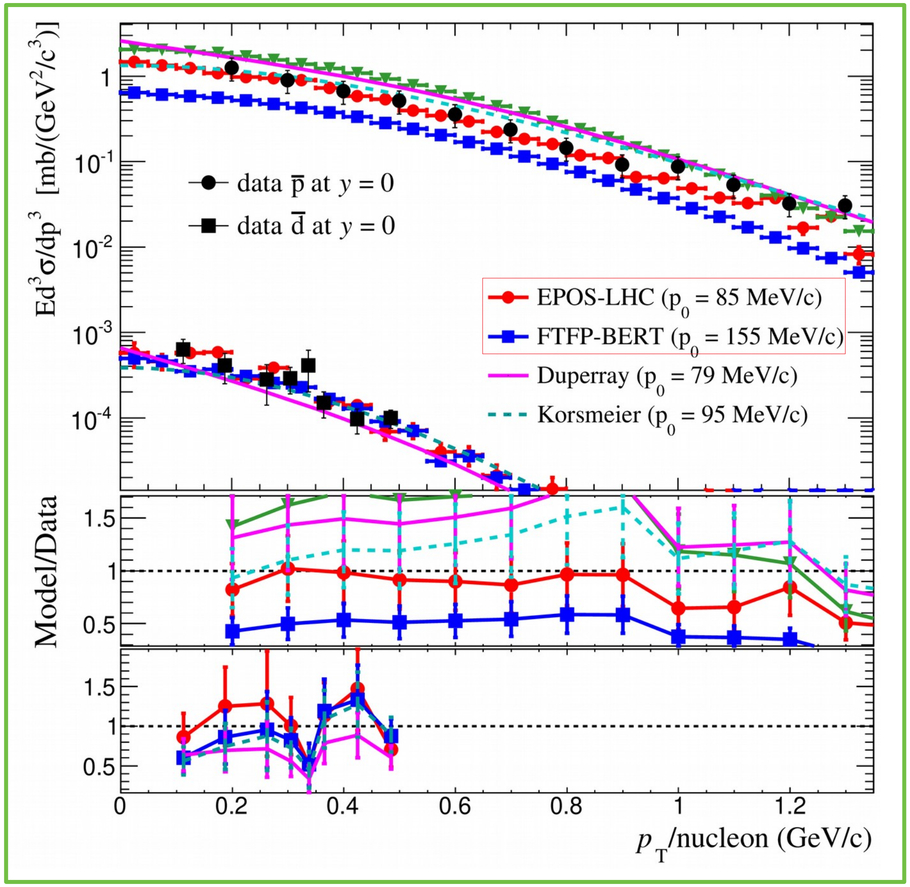

Antideuteron invariant differential cross section as function of p_T compared to ISR data.

p+p at √s = 900 GeV

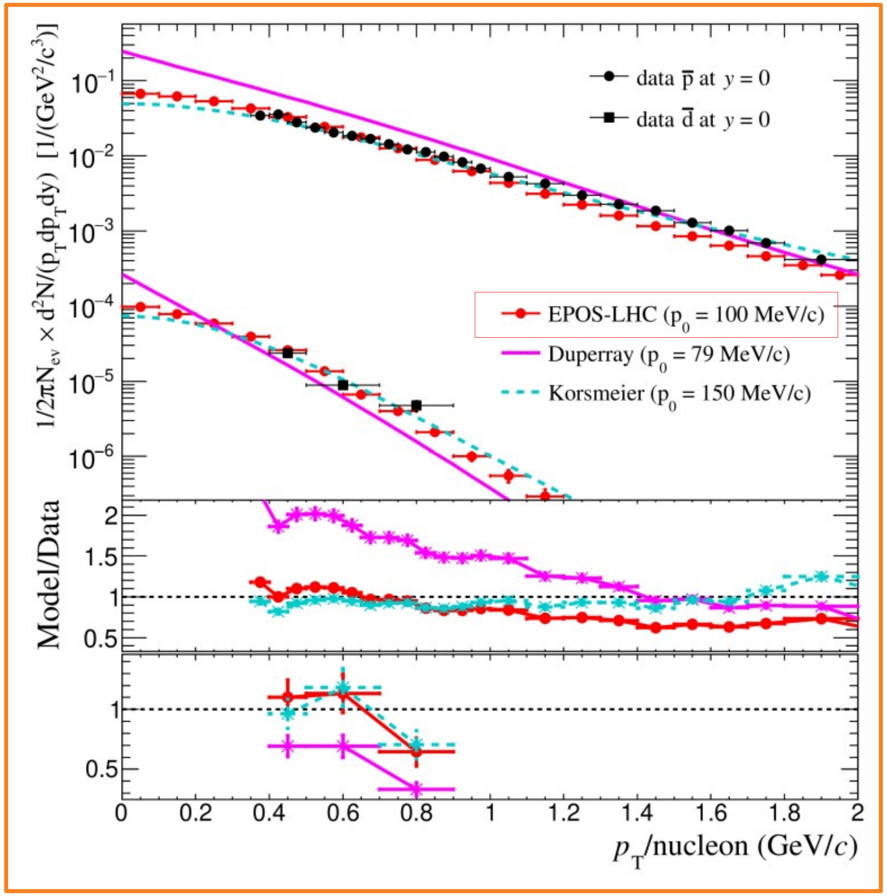

Antideuteron invariant differential cross section as function of p_T compared to ALICE-LHC data.

Coalescence momentum (p_0) and production cross section

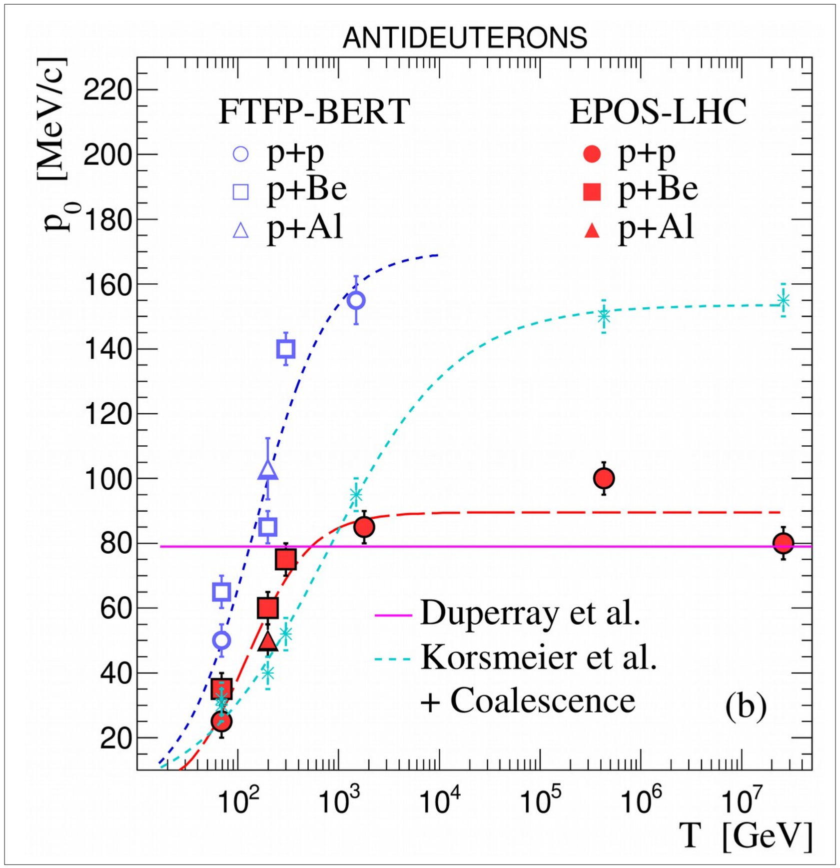

p+p → X + dbar

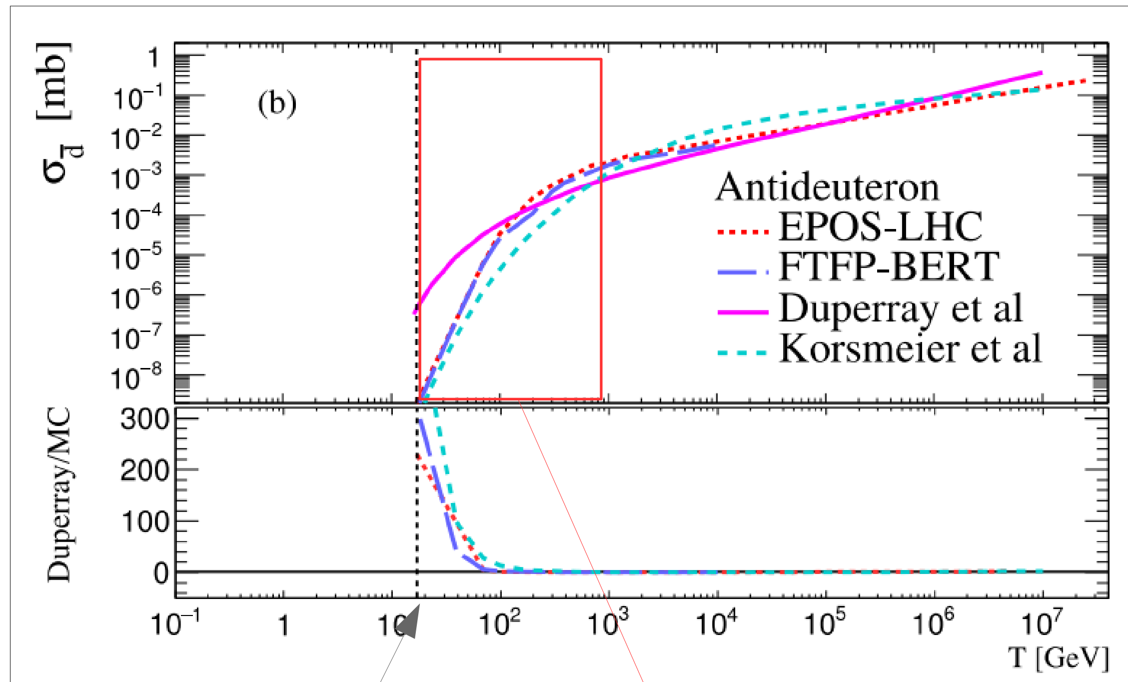

Energy production threshold

- p_0 is parameterized as function of the projectile kinetic energy.
- p_0 is similar for p+p and p+Be collisions.

- p_0 changes in the energy region of major importance for cosmic ray production.

Antihelium production simulation

- MC coalescence is expanded to merge 3 antinucleons from p-p interactions.
- High computing power is required ~ 2000 years so far.

- Using same p_0 as for dbar shows very good agreement with ALICE antihelium-3 data

p+p at √s = 7 TeV

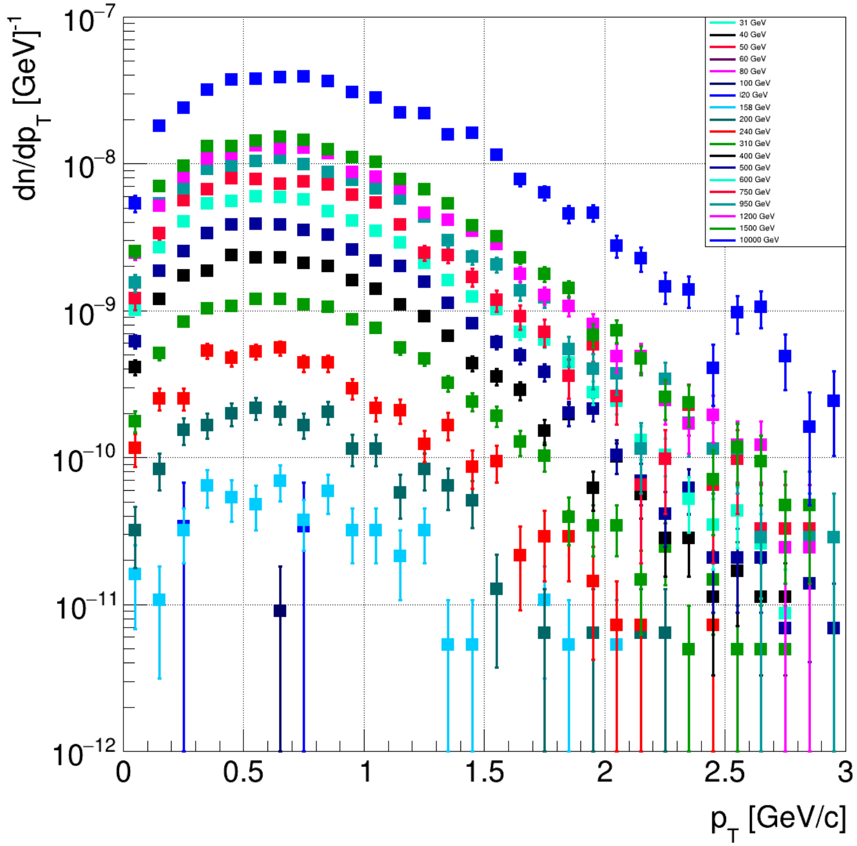

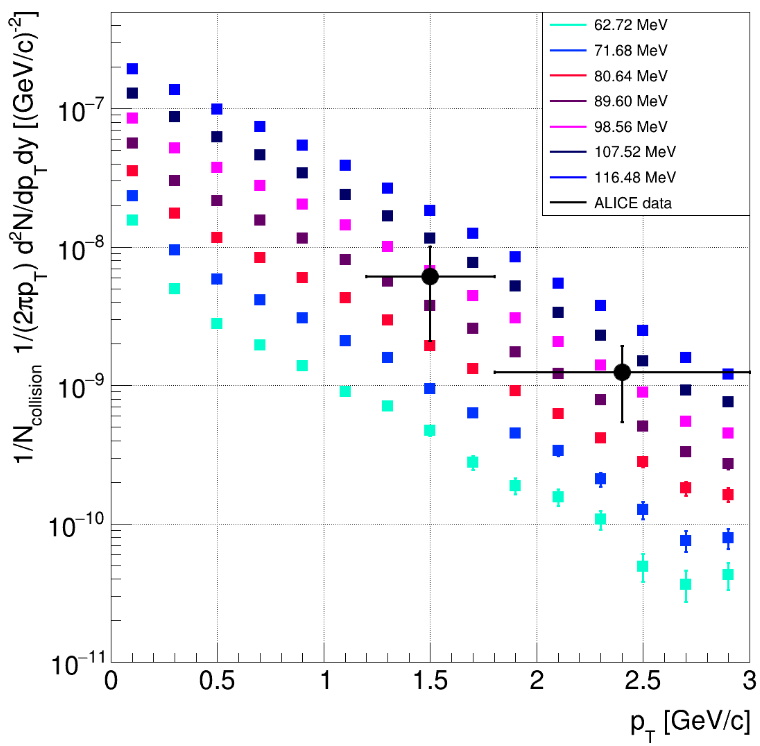

Anirvan Shukla PhD student UH

Propagation with Galprop56

$$\frac{\partial f(p,\vec{r},t)}{\partial t} = \vec{\nabla}\cdot\left(D_{xx}(p,\vec{r})\vec{\nabla}f - \vec{V}f\right) + \frac{\partial}{\partial p}p^2 D_{pp}\frac{\partial}{\partial p}\frac{1}{p^2}f - \frac{\partial}{\partial p}\left[\dot{p}f - \frac{p}{3}(\vec{\nabla}\cdot\vec{V})f\right] - \frac{1}{\tau_f}f - \frac{1}{\tau_r}f + q(p,\vec{r},t),$$

Antideuteron source term

Set 1 DR
Without convection

z [kpc]	$D_0/10^{28}$ [cm^2 s^{-1}]	δ	V_{alf} [km s^{-1}]
6	4.37	0.494	7.64

Proton

R1	R2	γ1	γ2	γ3
5.78 GV	304 GV	1.74	2.35	2.178

Helium

R1	R2	γ1	γ2	γ3
5.78 GV	304 GV	1.69	2.29	2.12

T. A. Porter et al., 2017

Set 2 DCR
With convection

z [kpc]	$D_0/10^{28}$ [cm^2 s^{-1}]	δ	V_{alf} [km s^{-1}]	V_{conv} [km s^{-1}]	dV/dz_{conv} [km s^{-1} kpc^{-1}]
4	4.3	0.395	28.6	12.4	10.2

Proton

R1	R2	γ1	γ2	γ3
7 GV	360 GV	1.69	2.44	2.28

Helium

R1	R2	γ1	γ2	γ3
7 GV	330 GV	1.71	2.38	2.21

M. J. Boschini et al 2017 PoS(ICRC2017)278

Antideuteron source term

$$q_{\bar{d}}^{sec}(E_{kin}^{\bar{d}}) = \sum_{i=p,He,\bar{p}} \sum_{j=p,He} 4\pi n_j \int_{T_{min}}^{\infty} dT_i \left(\frac{d\sigma}{dE_{kin}^{\bar{d}}}\right)_{ij} \Phi_i(T_i)$$

p, He Fluxes

EPOS-LHC cross-section

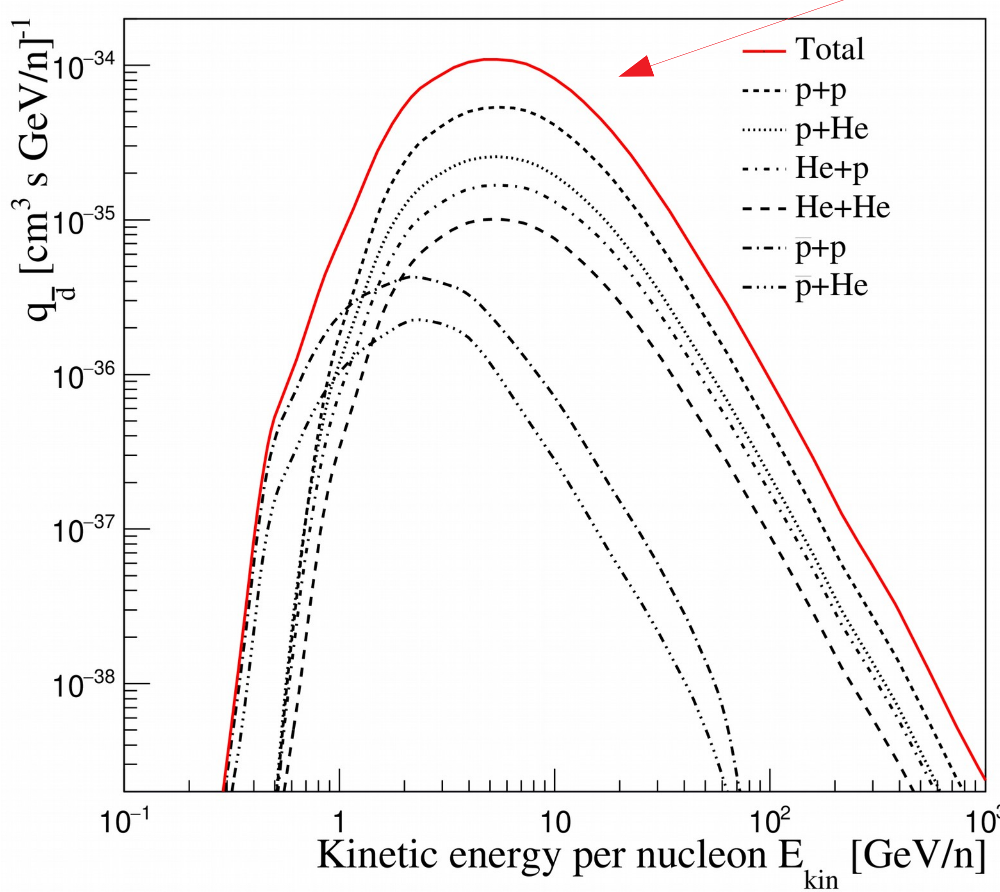

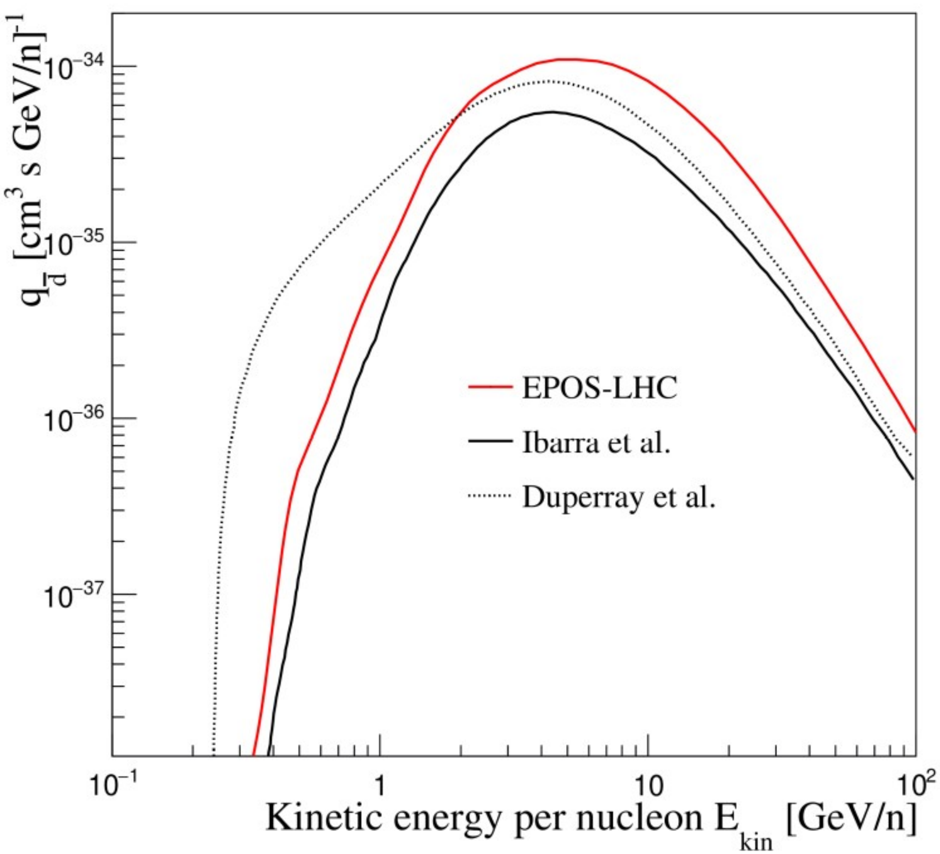

Proton and Helium fluxes

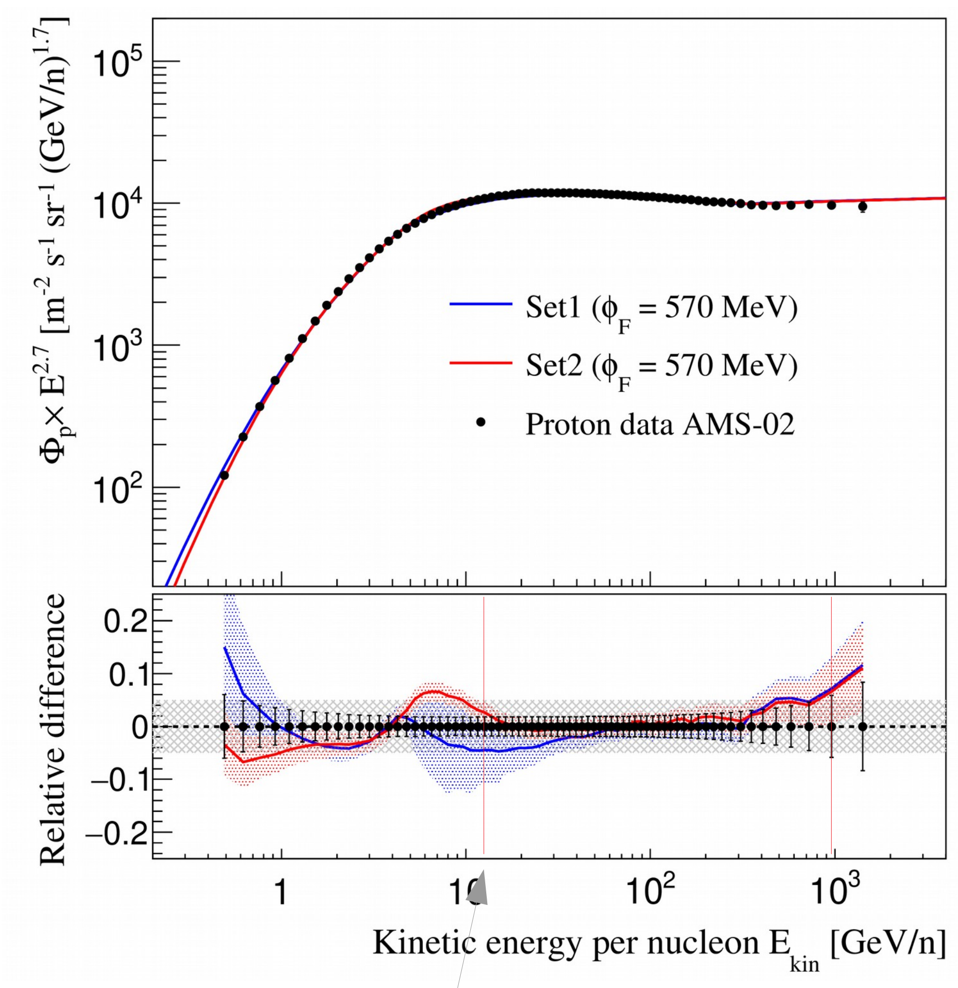

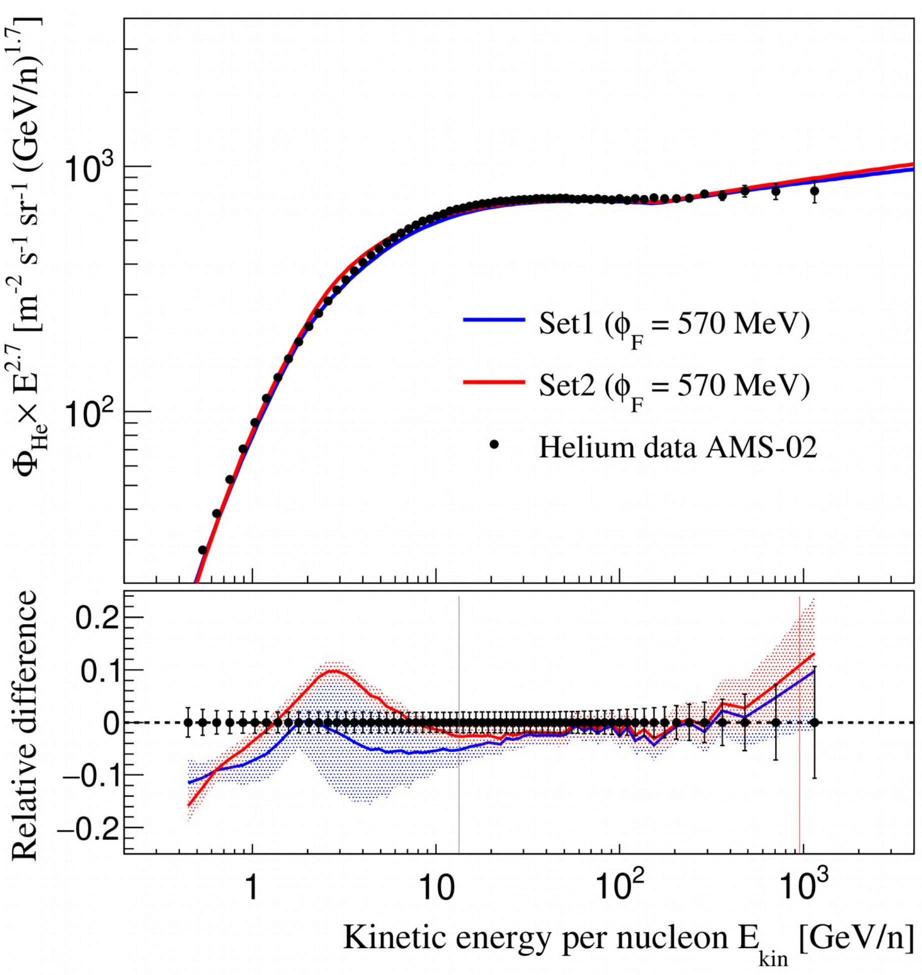

Energy production threshold

Secondary Antideuteron Flux

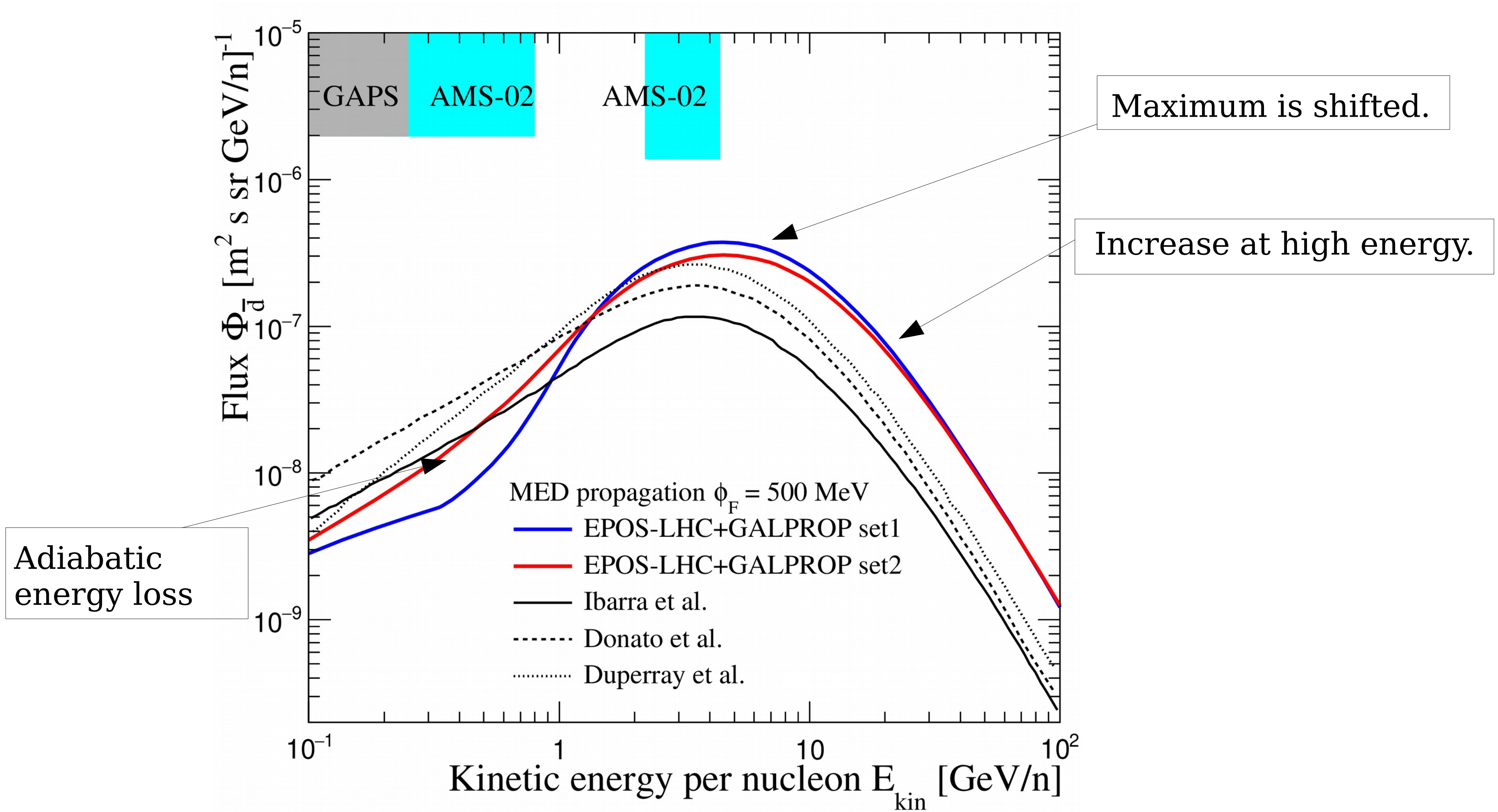

Summary

- A new study on the secondary antideuteron production was presented, using a high-energy MC generator (EPOS-LHC) and the coalescence model.

- Simulations were compared to an extensive data set, including new measurements from NA61 and ALICE-LHC to obtain the coalescence momentum (p_0).

- From the comparison to data, it seems the coalescence momentum (p_0) depends on the collision energy. As consequence:

  - Antideuteron production cross section shows important differences with respect to previous calculations in the region of interest for CR antideuteron production.

  - Antideuteron flux shape is slightly modified and its maximum is shifted above 4 GeV/n compared to other works.

  - Antideuteron flux is higher than previous estimations but it remains below experiment expected sensitivities.

Thank you!

Boron to Carbon ratio

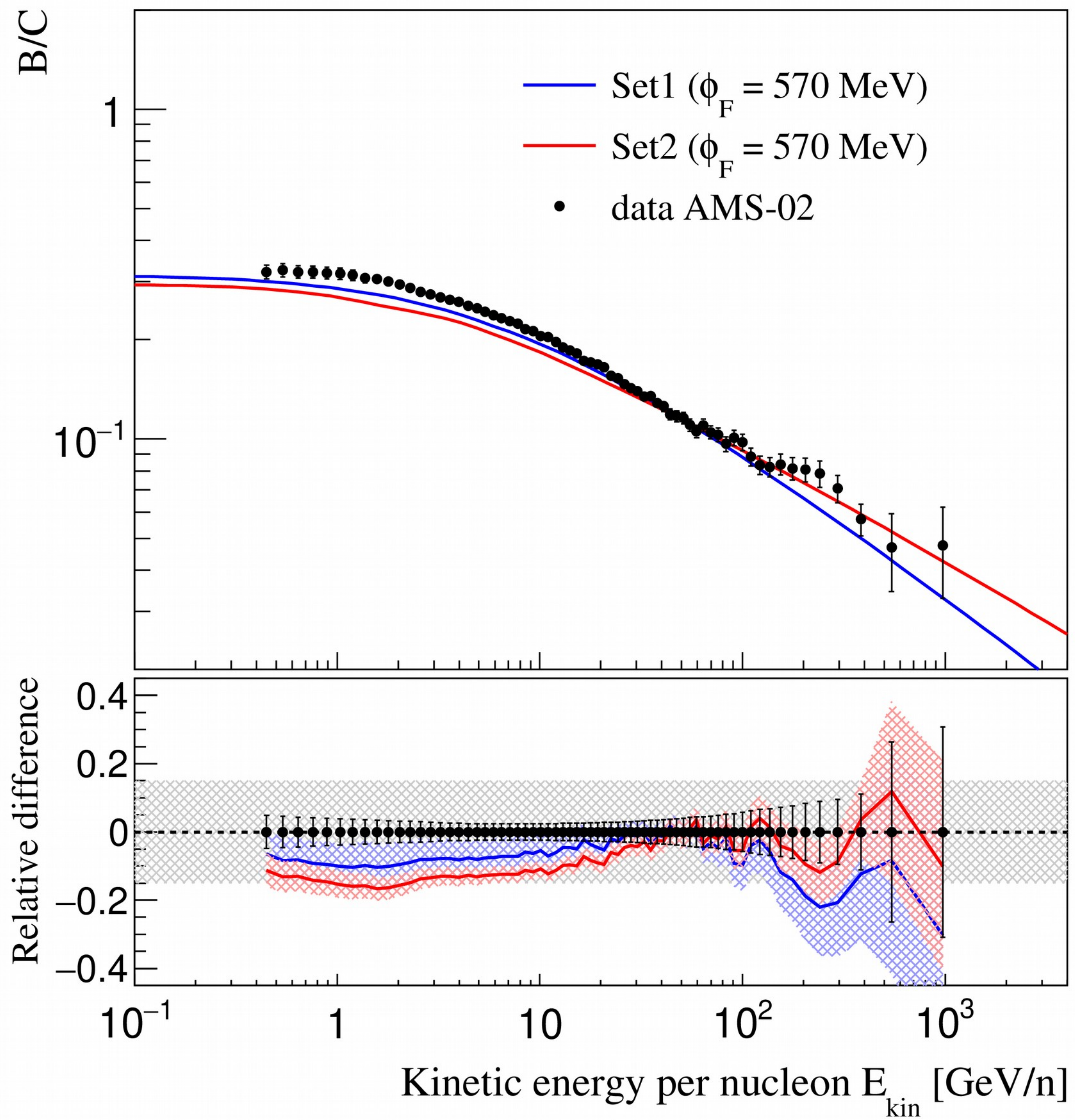

Antiproton production simulation

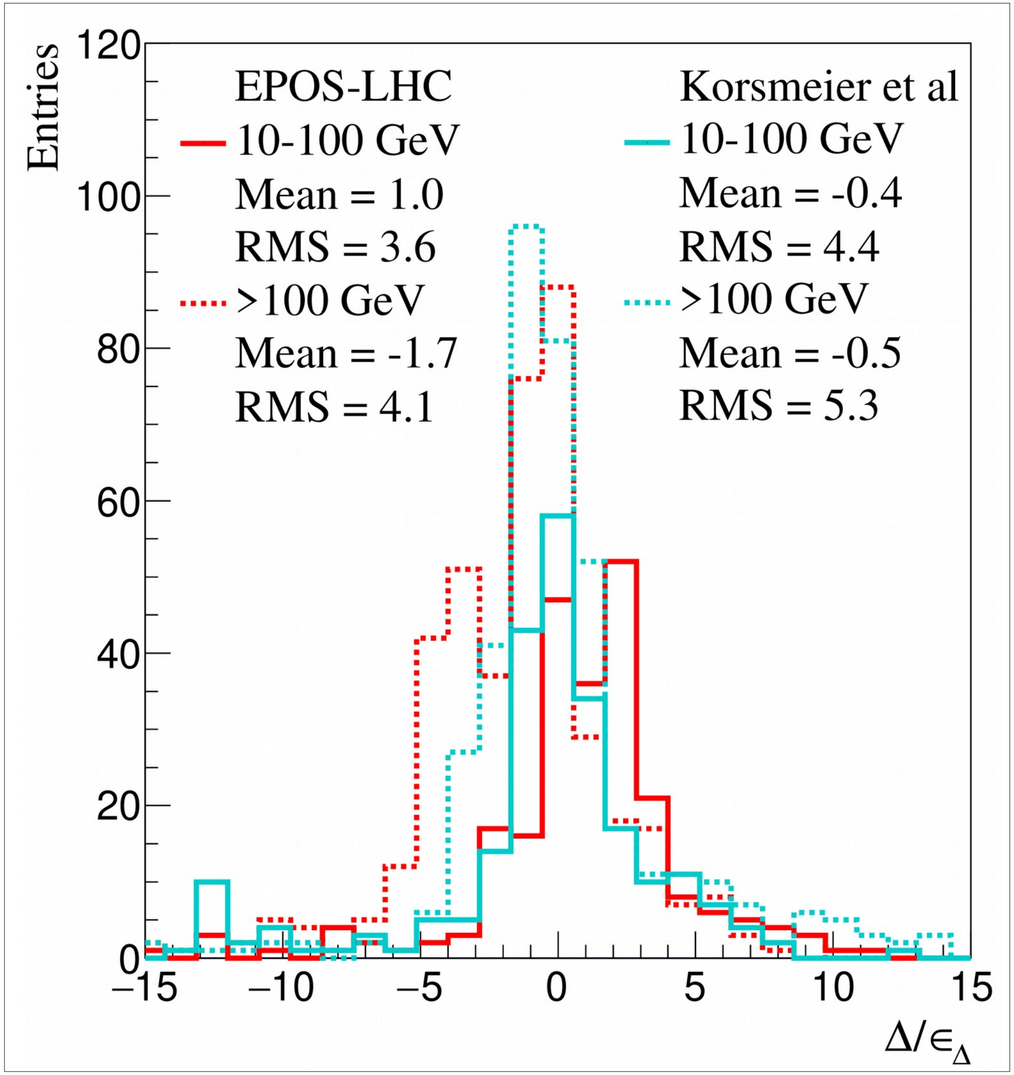

Antideuteron source term

- Proton and helium fluxes with and without hardening are inserted in the convolution.

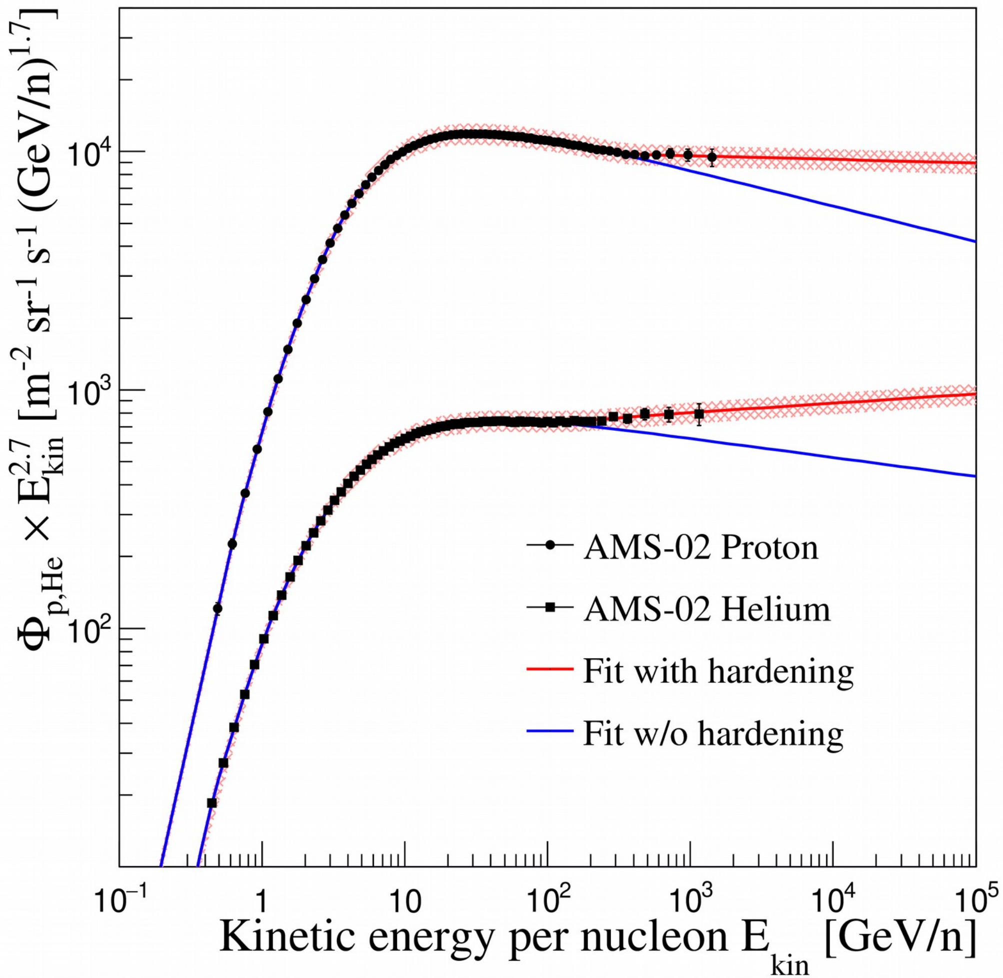

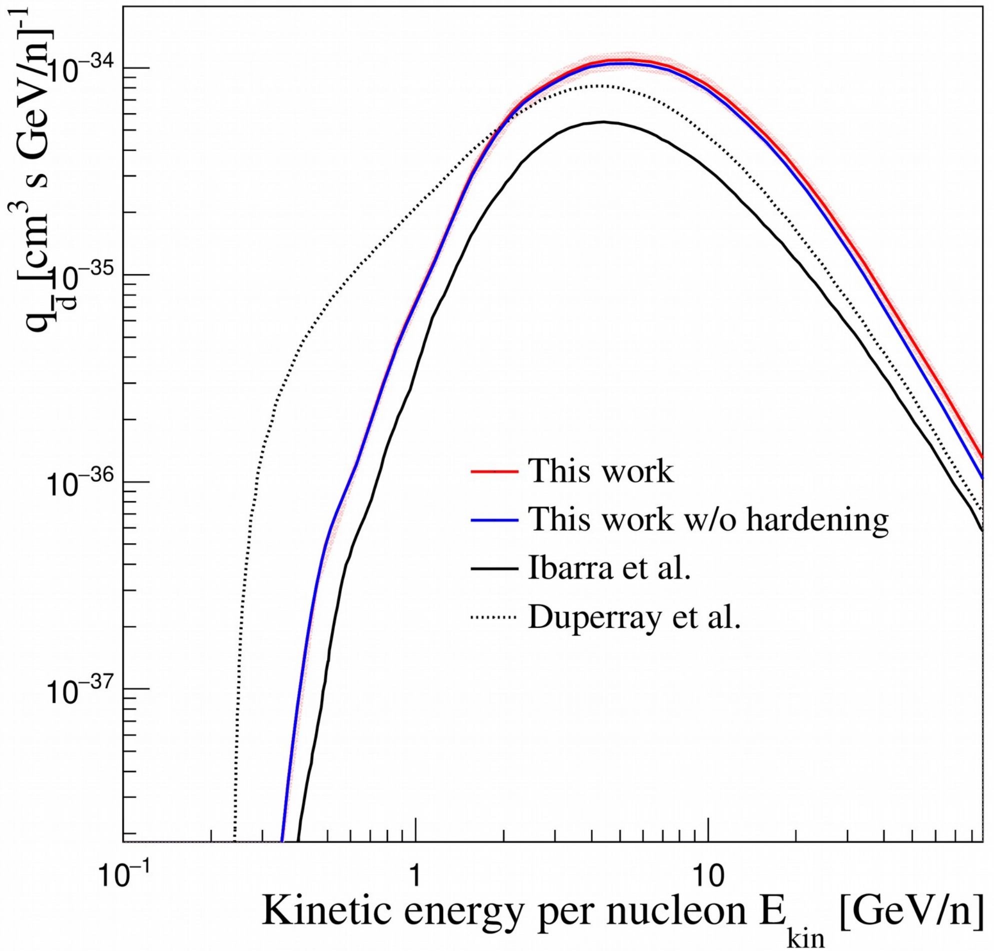

- Hardening increases dbar flux by less than 10%
- dbar production is higher than in previous works.